

Research Article

Inhibition Effects and Theoretical studies of Pyrazolidine-Diones as Corrosion Inhibitors for Mild Steel in 1M H₂SO₄ Solution

V.Hemapiya^{Å*}, P.Saranya^Å, K.Parameswari^Å and S.Chitra^Å^ÅDepartment of Chemistry, PSGR Krishnammal College for Women, Coimbatore – 4, Tamil Nadu, India

Accepted 05 Nov 2014, Available online 01 Dec 2014, Vol.4, No.6 (Dec 2014)

Abstract

Corrosion inhibition of mild steel in the presence of different concentrations of 1-phenylpyrazolidine-3,5-dione (PPD) and 4-(4-benzylidene)-1-phenylpyrazolidine-3,5-dione (BPP) in 1M H₂SO₄ solution has been studied using weight loss, potentiodynamic polarization and electrochemical impedance spectroscopy. The effect of temperature on the corrosion behavior of mild steel has been examined in the temperature range of 303–333 K. The inhibition efficiency increases with increasing inhibitor concentration but decreases with increasing temperature. The activation energy and free energy of adsorption for the inhibition reaction support the mechanism of physisorption. The adsorption of inhibitors on mild steel surface is endothermic, spontaneous and consistent with the Langmuir adsorption isotherm. Potentiodynamic polarization measurements indicate that PPD & BPP act as mixed inhibitors. Surface analysis of mild steel has been carried out using scanning electron microscopy (SEM) and Fourier transform infrared (FT-IR) spectroscopy which reveals the adsorption of inhibitors on mild steel surface. Quantum chemical calculations have been performed at B3LYP/6-31G(d,p) level to calculate the electronic properties of the molecules in order to complement the experimental results. The optimized structures, position of HOMO and LUMO of the molecules are obtained.

Keywords: Diones, corrosion, polarization, weight loss, adsorption, Density Functional theory (DFT), acid media.

1. Introduction

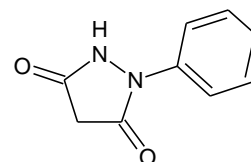
Mild steel is an important structural material used extensively in various industries. However, its tendency to corrode makes it unsuitable for exposure to acids. The use of inhibitors is one of the practical methods for protection against corrosion in acidic media. Heterocyclic compounds represent a potential class of corrosion inhibitors. Corrosion inhibition by nitrogen containing heterocyclic compounds has been widely reported in literature (Granese S L *et al*, 1992; Subramaniam G *et al*, 1990; Hettiarachchi S *et al*, 1989; Stupnisek- Lisac E *et al*, 1992; Raicheva S *et al*, 1993). Pyrazolidine -3,5-diones are most important derivatives of pyrazole and are present as a basic moiety in a number of pharmaceutical compounds like phenylbutazone, oxyphenbutazone and novalgin (Harish Kumar and Sandeep Jain, 2013). Survey of literature reveals that pyrazoles and their derivatives are studied as effective corrosion inhibitors (HuiCang *et al*, 2012; Mehdi Ebadi *et al*, 2012; L. Herrag *et al*, 2008), but the corrosion inhibitive performance of pyrazolidine -3,5-diones is scanty. This work deals with the inhibition behavior of 1-phenylpyrazolidine-3,5-dione (PPD), and 4-(4-benzylidene)-1-phenylpyrazolidine-3,5-dione (BPP) on mild steel in acid media.

2. Experimental work

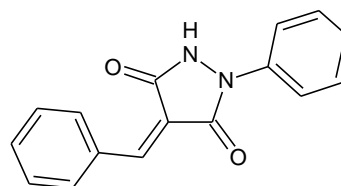
*Corresponding author: V.Hemapiya

Material

Cold rolled mild steel with elemental composition of: C=0.079%, P=0.025%, Mn=0.018%, S=0.021% and the rest Fe was used for the study. Rectangular specimens with dimension 3 cm X 1 cm x 0.05 cm were used. The plates were abraded with fine grade of emery papers, degreased with acetone, washed with double distilled water, dried and used for the entire immersion studies.



PPD



BPP

All reagents used for the study were analar grade and double distilled water was used for their preparation. Pyrazolidine-3,5-diones were synthesized from

diethylmalonate and phenyl hydrazine by the reported procedure (Harish Kumar and Sandeep Jain,2013).

2.1 Weight loss method

The pretreated mild steel specimens were initially weighed and immersed in 1M H₂SO₄ with various concentrations of the inhibitors and without inhibitor for three hours at 30± 1°C. The specimens were taken out, washed thoroughly with distilled water, dried and the final weights were noted to determine the weight loss. From the weight loss, the corrosion rate (mpy), inhibition efficiency (%) and surface coverage (θ) were calculated using the formula,

$$CR = 534 \times W / DAT, \quad (1)$$

$$IE (\%) = [W_0 - W_i / W_0] \times 100 \quad (2)$$

$$\theta = [W_0 - W_i / W_0] \quad (3)$$

Where W- Weight loss in milligrams(mg), D-Density in grams per cubic centimeter(g/cm³),A-Area of specimen exposed in square inches, T-Time of immersion in hours (h) and W₀ and W_i - Weight loss (in g) of mild steel in the absence and presence of inhibitor respectively. In order to study the influence of temperature on protection efficiency, the above procedure was followed in the absence and presence of inhibitors at higher temperatures with 0.25mM concentration of inhibitors.

2.2 Electrochemical studies

The electrochemical measurements were carried out in a glass cell with a capacity of 100ml. A platinum electrode and saturated calomel electrode were used as counter electrode and reference electrode respectively. The mild steel electrode in the form of cylindrical rod embedded in Teflon with an exposed area 0.785cm² was used as working electrode. The EIS measurement was made at a corrosion potential over a frequency range of 0.01Hz to 10 KHz with signal amplitude of 25 mV. The Tafel polarization were made after EIS for a potential range of -200mV to +200 mV with respect to open circuit potential, at a scan rate of 1mV/sec.

2.3 Synergistic effect of halide ions

The synergistic effect was studied by the addition of 1mM KI to the mild steel specimen immersed in 1M H₂SO₄ containing various concentrations of the inhibitors for a duration of three hours. From the weight loss data, the corrosion rate and inhibition efficiency were calculated. The same procedure was repeated with KCl and KBr.

2.4 Surface analysis

The surface morphology of the corroded and inhibited coupons was analyzed by Scanning Electron Microscope (SEM) and Atomic Force Microscopy (AFM). FT-IR spectra were recorded for the inhibitors and also for corrosion products scratched from mild steel plate immersed in 1M H₂SO₄ with and without inhibitors.

2.5 Computational chemistry

The molecular sketches of PPD and BPP were drawn using the Gaussian 09 program. All the quantum chemical calculations were performed using DFT method at B3LYP/6-31G(d,p) level. Total energy, dipole moment, charge density, energies of highest occupied (HOMO) and lowest unoccupied (LUMO) molecular orbital were examined to evaluate the corrosion inhibition efficiency of the studied inhibitors.

3. Results and discussion

3.1 Weight Loss Method:

The inhibition efficiency of the inhibitors (PPD & BPP) at various concentrations for mild steel corrosion in 1M H₂SO₄ has been evaluated by weight loss measurements and the results are summarized in Fig-1. The inhibition efficiency increases with increase in concentration of the inhibitors at the same time the corrosion rate decreases. This may be due to the adsorption of inhibitors on the metal surface making a barrier film for mass and charge transfer thus protecting the metal surface from corrosion. The adsorption of inhibitors on mild steel surface may be due to the interaction between the electrons of aromatic rings and free pairs of electrons over oxygen and nitrogen atoms with the positively charged metal surface.

3.1.1 Effect of temperature

The temperature performance (303 – 333 K) of the inhibitors at 0.25mM concentration is depicted in Fig-2 and the corresponding Arrhenius plots are shown in Fig-3. Fig-2 reveals that inhibitor efficiency decreased with increase in temperature. This may be due to the less protective nature of the inhibitive film formed on the mild steel surface at higher temperatures because of desorption of the inhibitor molecules from the metal surface. The activation thermodynamic parameters of the corrosion reaction such as the energy E_a, the entropy ΔS° and the enthalpy ΔH° of activation, were calculated from Arrhenius Eq. (4) and its alternative formulation called transition state Eq. (5).

$$\text{Corrosion rate} = k \exp (-E_a/RT) \quad (4)$$

$$\text{Corrosion rate} = \frac{RT \exp(\Delta S)}{Nh} \exp \left(\frac{-\Delta H}{R} \right) \quad (5)$$

Where k is the Arrhenius pre-exponential constant, E_a is activation energy for the corrosion process, R is the universal gas constant and h is the Planks constant. A plot of log corrosion rate Vs 1/T (Fig-3) was found to be linear with a correlation coefficient of ≈0.99. The activation energy values, (E_a) computed from the Arrhenius slopes for uninhibited and inhibited systems (Table-1) shows that the activation energy is higher in the presence of inhibitor. An increase in E_a suggests physical adsorption. A plot of log corrosion rate/T as a function of 1/T (Fig-4) was made. Straight lines were obtained with slope (-ΔH/2.303 RT) and intercept [(log (R/Nh) + (ΔS/2.303RT))] from which

Table 1: The free energy of adsorption of inhibitors at various temperature and activation energy of the inhibitors

Inhibitor	Ea (kj)	ΔG_{ads}° At Various Temperatures (KJ)				ΔH J/mol/K	ΔS KJ/mol
		303 K	313 K	323 K	333 K		
Blank	6.844	-	-	-	-	1.82	-43.35
PPD	25.84	-19.03	-18.56	-18.18	-17.49	10.07	-23.87
BPP	17.19	-17.28	-17.30	-17.68	-16.78	6.31	-34.58

Table 2: Corrosion parameters for mild steel at selected concentration of the inhibitors in 1M H₂SO₄ by potentiodynamic polarization method at 30 ± 1°C

Inhibitor	Concentration (mM)	Tafel slopes (mV/decade)		E _{corr} (mV)	I _{corr} (μ A/Cm ²)	IE (%)
		b _c	b _a			
PPD	Blank	55	121	-473.6	3210	-
	0.05	59	135	-490.2	2859	10.93
	0.15	56	147	-482.3	2564	20.12
	0.25	53	141	-478.8	1907	40.59
BPP	0.05	65	137	-500.8	600	85.36
	0.15	62	147	-485.5	531	87.04
	0.25	55	137	-478.4	236	94.24

Table 3: AC impedance parameters for mild steel at selected for mild steel at selected concentrations of the inhibitors in 1M H₂SO₄

Inhibitor	Concentration (mM)	R _i (ohm/cm ²)	C _{dl} (μ F/Cm ²)	Inhibition efficiency (%)
PPD	Blank	6.18	972.31	-
	0.05	13.43	401.92	53.98
	0.15	16.23	350.399	61.92
	0.25	20.68	246.79	70.11
BPP	0.05	42.59	106.82	85.48
	0.15	56.08	84.75	88.98
	0.25	68.27	85.75	90.94

Table 4: Synergistic effect of 1mM KCl/KBr/KI on the inhibition efficiency of inhibitors in 1M H₂SO₄ by weight loss method at 30±1°C

Inhibitor	Concentration (mM)	Inhibition Efficiency (%)			
		Without KCl/KBr/KI	With 1mM KCl	With 1mM KBr	With 1mM KI
PPD	0.01	15.04	34.68	56.2	65.43
	0.03	19.38	46.08	67.45	71.20
	0.05	23.69	52.35	69.06	74.23
	0.07	31.81	66.43	70.02	79.40
	0.09	39.49	69.78	75.29	83.28
BPP	0.01	17.19	41.89	57.85	63.68
	0.03	22.22	47.36	61.32	65.36
	0.05	34.14	52.36	69.49	73.47
	0.07	40.82	60.03	75.36	84.44
	0.09	44.68	69.36	79.58	92.01

Table 5: Quantum chemical parameters calculated using B3LYP/6-31G(d,p)

Parameters	PPD	BPP
E _{HOMO} (eV)	-6.0600	-5.8401
E _{LUMO} (eV)	-0.9066	-2.5584
ΔE (eV)	5.1533	3.2817
Dipole moment (Debye)	2.1432	1.3205
IP (eV)	6.0600	5.8401
EA (eV)	0.9066	2.5584
σ	0.3880	0.6904
χ (eV)	3.4833	4.1992
η	2.5767	1.6408
Total energy	-607.71	-876.86
Molar volume(cm ³ /mol)	121.15	163.157

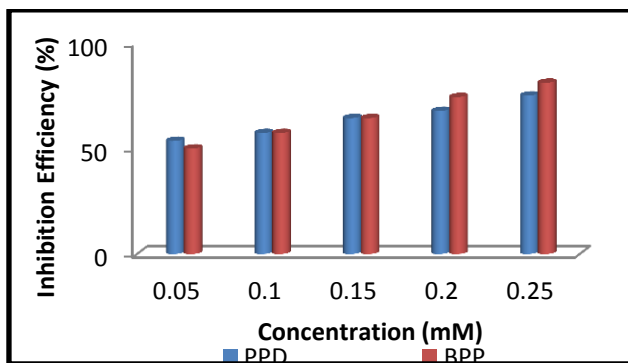


Figure 1: Variation of inhibition efficiency with concentration for the inhibition of corrosion of mild steel in 1M H₂SO₄

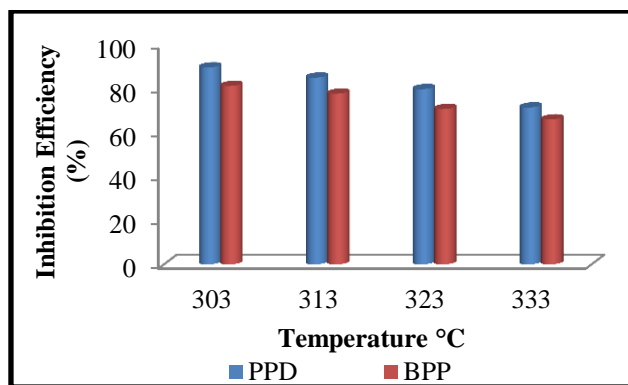


Figure 2: Variation of inhibition efficiency with temperature for the inhibition of corrosion of mild steel in 1M H₂SO₄

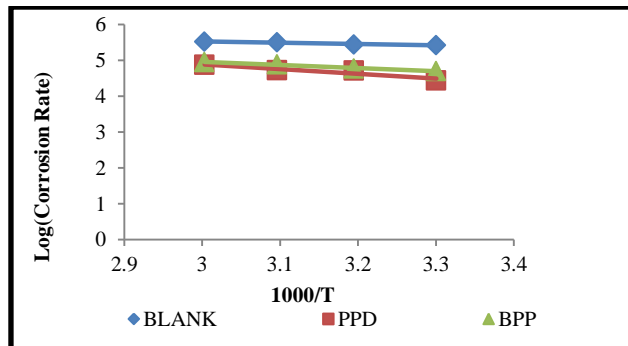


Figure 3: Arrhenius plot of corrosion rate of mild steel in 1M H₂SO₄ in presence and absence of the inhibitors

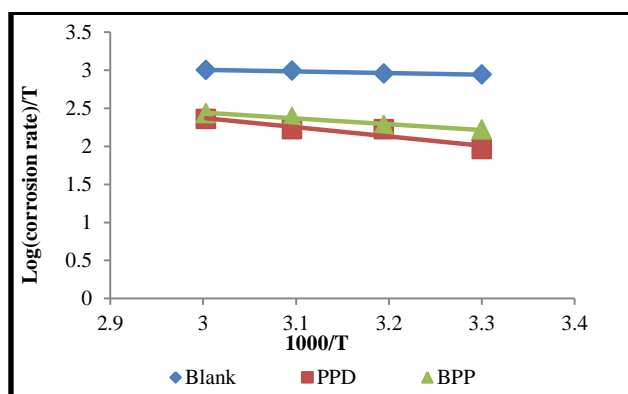


Figure 4 Plot of log (corrosion rate/T) Vs 1/T for corrosion of mild steel in 1M H₂SO₄ in presence and absence of the inhibitors

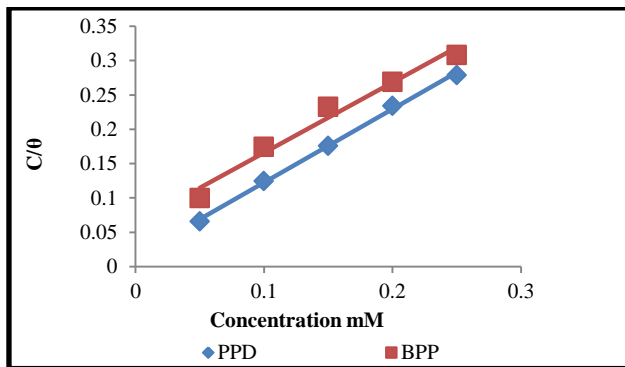


Figure 5: Langmuir's adsorption isotherm plots for corrosion of mild steel in 1M H₂SO₄

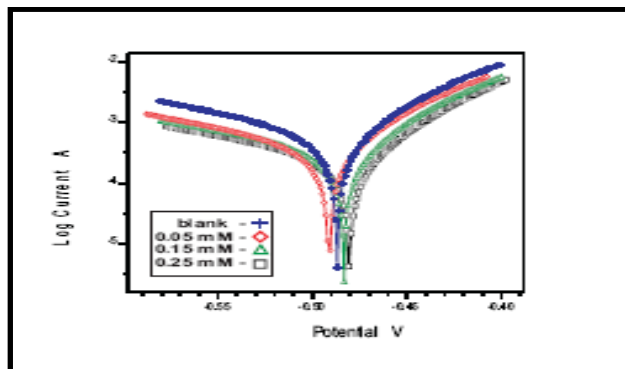


Figure 6: Polarization curve for mild steel in 1M H₂SO₄ in presence and absence of the BPP

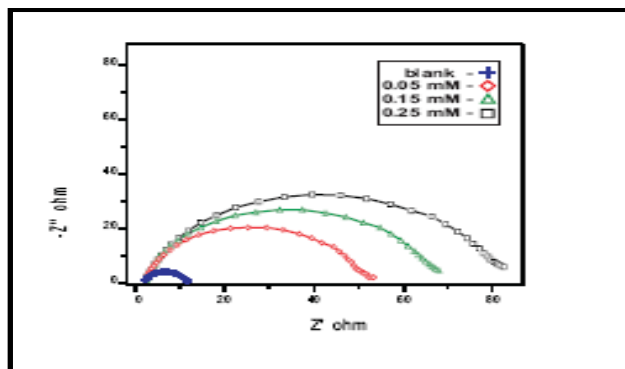
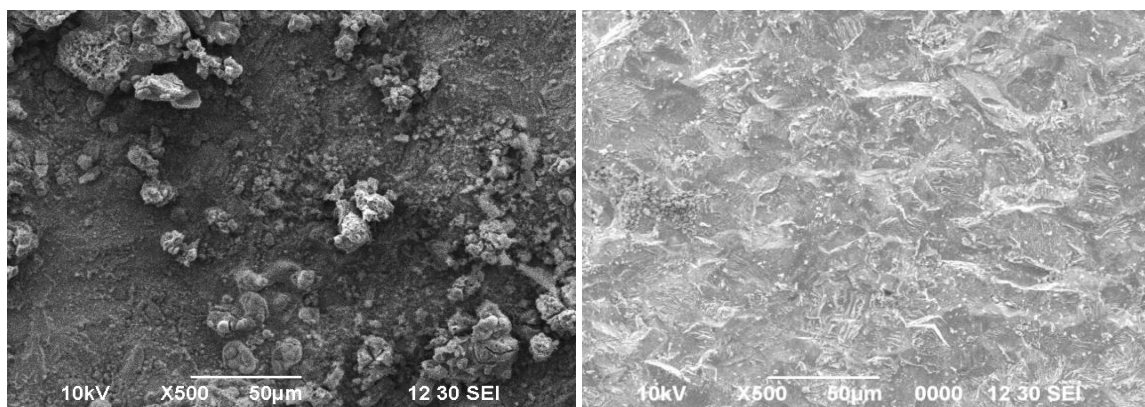


Figure 7: Nyquist diagram for mild steel in 1M H₂SO₄ in presence and absence of the BPP



(a)

(b)

Figure 8: SEM micrograph of mild steel in the absence and presence of BPP

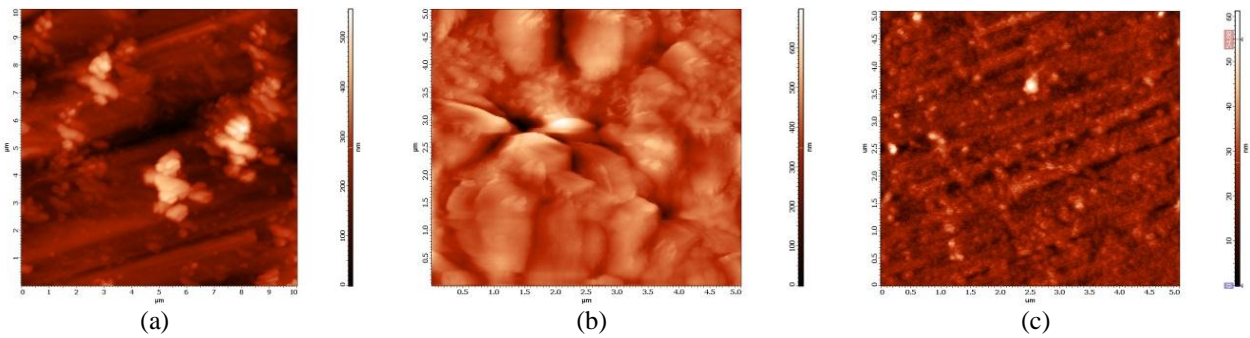


Figure 9: Two dimensional AFM image of mild steel (a) polished (b) in 1M H₂SO₄ (c) presence of BPP

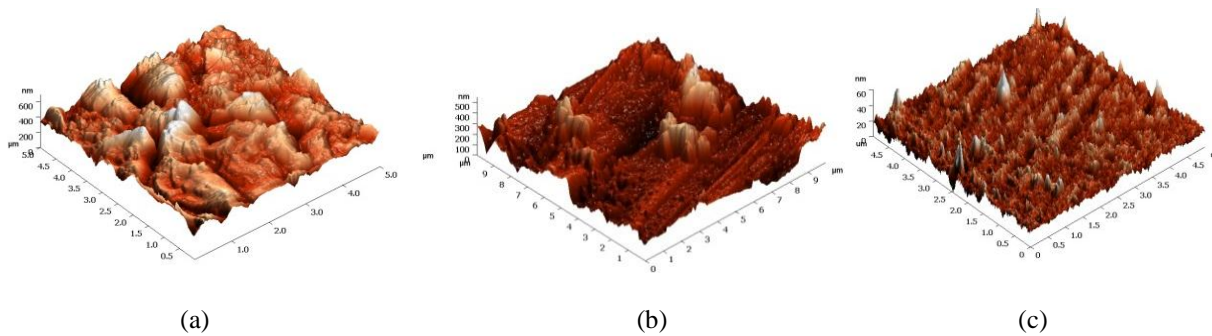


Figure 10: Three dimensional AFM image of mild steel (a) polished (b) in 1M H₂SO₄ (c) presence of BPP

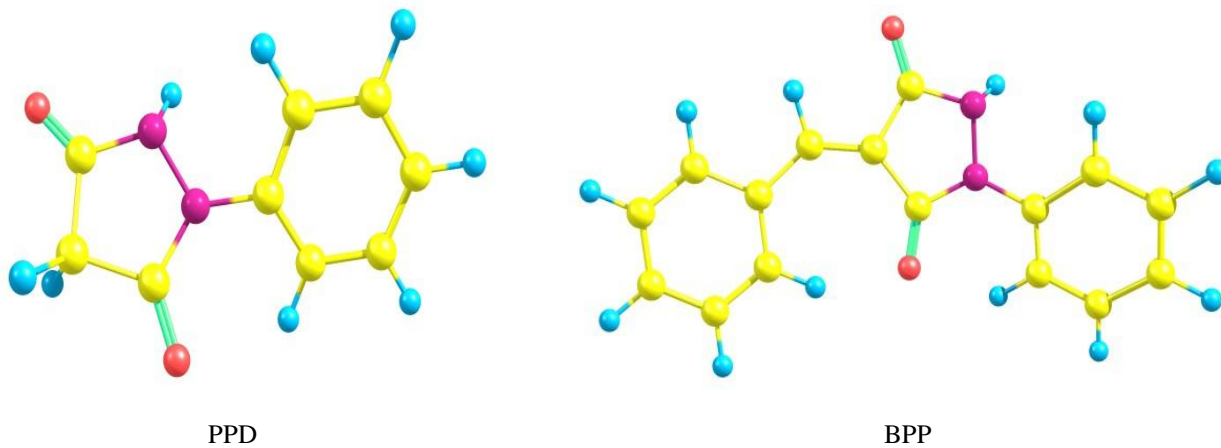


Figure11: Optimized structure of the inhibitors

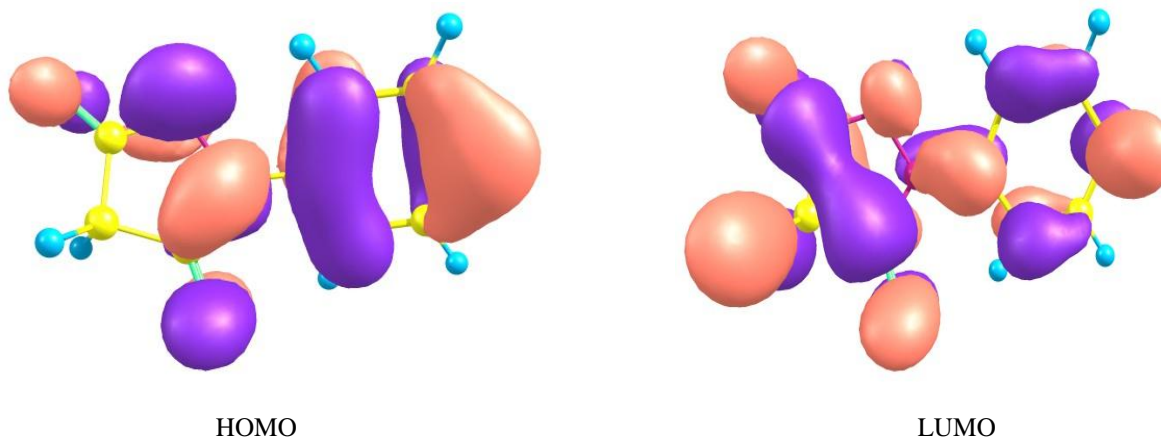


Figure12a: Homo & Lumo of PPD

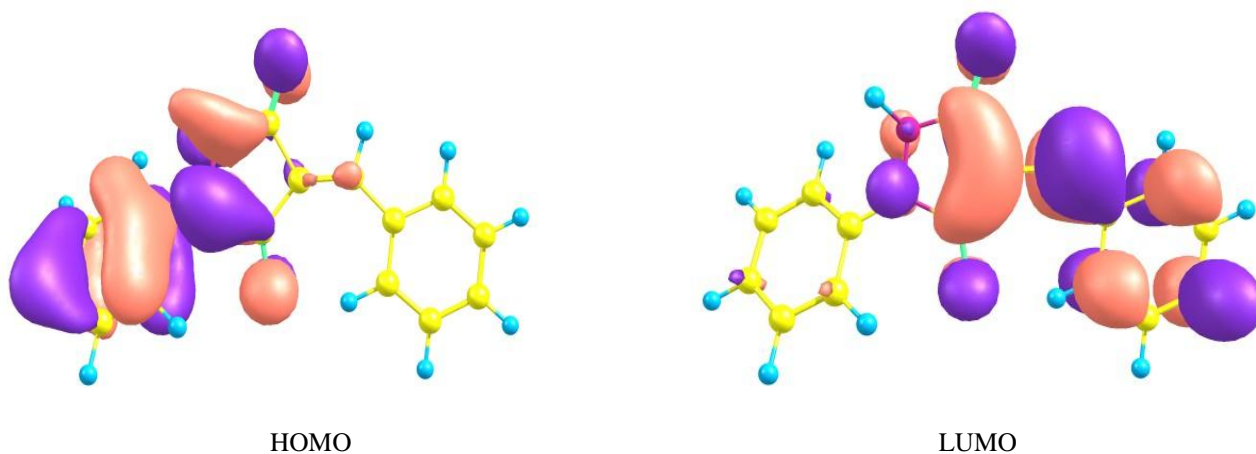


Figure 12b: Homo & Lumo of BPP

the values of ΔH and ΔS , respectively were calculated and given in Table 1. The positive values of ΔH implies endothermic nature of metal dissolution process. The negative values of ΔS indicate that a decrease in disorderliness on going from reactant to product.

3.1.2 Adsorption isotherm

In order to get better understanding of the adsorption mode of inhibitors on the mild steel surface, the surface coverage obtained from weight loss data were tested graphically by fitting to various isotherms. The value of correlation coefficient (R^2) was used to determine the best fit isotherm. Langmuir isotherm was found to fit well with the experimental data. table

$$(C/\theta) = (1/K_{ads}) + C \quad (6)$$

The plots of (C/θ) versus C gave straight lines (Fig-5) with R^2 values close to unity indicating strong adherence of the adsorbed inhibitors to the assumptions of Langmuir (Ali S A et al, 2003).

3.2 Electrochemical studies

3.2.1 Polarization studies

Polarization behavior of mild steel immersed in 1M H_2SO_4 at $30 \pm 1^\circ C$ in the absence and presence of different concentrations of the inhibitors was studied and the corrosion kinetic parameters such as corrosion potential (E_{corr}), corrosion current density (I_{corr}), Tafel constants (b_a & b_c) derived from the experiment are listed in Table-2. Potentiodynamic polarization curve of BPP is depicted in Fig-6. I_{corr} value decreases in the presence of inhibitor compared to that in the absence of inhibitor and also decreases with increase in inhibitor concentration. From the table it is observed that presence of inhibitor does not shift E_{corr} remarkably indicating that the inhibitors act as mixed type affecting both anodic dissolution and cathodic hydrogen evolution reaction. Cathodic and anodic Tafel slopes also confirm that the inhibitors act as mixed type.

3.2.2 EIS studies

The corrosion behavior of steel, in acidic solution in the absence and presence of different concentrations of the

inhibitors was investigated by electrochemical impedance spectroscopy at 303K. Typical Nyquist plot obtained for BPP is shown in Fig-7. The semicircular nature of the plot indicates the formation of a barrier film on the surface and a charge transfer process mainly controlling the corrosion of mild steel. The diameter of the semicircle increases with inhibitor concentration. The charge transfer resistance (R_t) and the double layer capacitance (C_{dl}) obtained from impedance measurements are given in Table-3. The impedance of the inhibited mild steel increases with increase in inhibitor concentration and consequently the inhibition efficiency increased. Decrease in C_{dl} which can result from a decrease in local dielectric constant and /or an increase in the thickness of electrical double layer suggests that the inhibitor molecules act by adsorption at metal/solution interface (Prabhu R A et al, 2008). This indicated the formation of a protective film of the inhibitor on the surface.

3.3 Synergistic effect of halide ion

The synergistic effect provided by the addition of halide ions such as I^- , Br^- and Cl^- to the solution containing 1M H_2SO_4 and the inhibitors was studied by weight loss method and the data are presented in Table-4. Analysis of the data reveals that the addition of halides to the inhibitors increases the inhibition at each concentration of the inhibitor tested. Synergistic ability of the halide ion increases in the order $Cl^- < Br^- < I^-$. The greater influence of the iodide ion is attributed to the larger ionic radius, low electro negativity and high hydrophobicity as compared to other halides (Umoren S A, Ebenso E E, 2007).

3.4 Surface Analysis

3.4.1 Scanning Electron Microscopy

SEM images of mild steel surface immersed in inhibited and uninhibited 1M H_2SO_4 is shown in Fig-8(a & b). Inspection of the SEM micrographs showed that the surface of mild steel became rough in the absence of inhibitor (8a) and became relatively smooth with deposited inhibitors in the presence of 0.25mM BPP (8b). This confirms the corrosion inhibition of mild steel by BPP through adsorption of inhibitor molecules on the metal surface.

3.4.2. Atomic adsorption Microscopy

To establish whether inhibition is due to the formation of adsorbed film on the metal surface, atomic force micrographs were taken. The two dimensional and three dimensional AFM micrographs are shown in Fig- 9(a-c) and 10(a-c) respectively. The average roughness of the polished mild steel (Fig-10a) and mild steel in 1M H₂SO₄ solution without inhibitor (Fig-10b) was calculated as 31 and 69 nm, respectively. The mild steel surface in the free acid solution is getting cracked due to the acid attack on the surface. However, in presence of 0.25mM BPP (Fig-10c), the average roughness was reduced to 42 nm. These results confirm that corrosion inhibition is due to the formation of a protective film by the adsorption of inhibitors on mild steel surface.

3.5 Computational Chemistry

Recently quantum chemical calculations have been widely used to study the reaction mechanisms. To investigate the effect of structure on the inhibition mechanism and efficiency, theoretical calculations were performed. The optimized geometry and Frontier molecular orbitals are shown in Fig-11. The calculated quantum chemical parameters necessary for discussion on the reactivity of the studied compounds are presented in Table 5.

The energy of the highest occupied molecular orbital (E_{HOMO}) measures the tendency towards the donation of electron by a molecule (H.E. El Ashry *et al*, 2006). Therefore high E_{HOMO} values indicate better tendency towards the donation of electron, enhancing the adsorption of the inhibitor on mild steel surface and hence better inhibition efficiency. It is evident from the data presented in Table -5 that BPP is the best inhibitor with high E_{HOMO} values. This indicates that BPP is better adsorbed on mild steel surface via electron donation compared to PPD. The energy of the lowest unoccupied molecular orbitals indicates the ability of the molecule to accept electrons. Lower the value of E_{LUMO} , the more probability of the molecule to accept electrons. Therefore, the lower the value of E_{LUMO} the better is the expected inhibition efficiency. The energy gap ($\Delta E = E_{\text{HOMO}} - E_{\text{LUMO}}$) of the molecule represents the softness or hardness of the molecule. Obi-Egbedi *et al*, (2011) reported that a hard molecule has a large energy gap and a soft molecule has a small energy gap. According to Ebenso *et al*, (2010) the inhibitor with least value of hardness is expected to have the highest inhibition efficiency. For the simplest electron transfer, adsorption could occur on the part of the molecule where softness, which is a local property, has a highest value (Hasanon R *et al*, 2007). In the present study BPP with low ΔE (3.2817eV) and softness 0.6904 has the highest inhibition efficiency. Molecular volume indicates possible surface coverage of metal by the inhibitor. The larger the molecular volume, greater is the inhibition efficiency because of increased surface coverage. The large molecular volume of BPP indicates its higher protection efficiency compared to PPD.

3.5 Mechanism of Inhibition

The corrosion inhibitive performance of organic inhibitors in acidic medium is explained on the basis of adsorption.

The first step in the inhibitive mechanism is adsorption of inhibitors at the metal solution interface. In aqueous acid solutions the pyrazolidine diones exist either as neutral molecules or protonated species get adsorbed on the metal solution interface by one or more of the following ways: (1) electrostatic interaction between the charged molecules and charged metal, (2) interaction of unshared electron pairs in the molecule with vacant d orbitals of surface metal atoms, (3) interaction of π electrons of aromatic ring with vacant d-orbitals of surface metal atoms and (4) a combination of above (H.M.Bhajiwal *et al*, 2001). In the present study the experimental data shows physical adsorption of inhibitors which requires presence of both electrically charged surface of the metal and charged species in the bulk of the solution; the presence of metal having low- energy electron orbital and an inhibitor with molecules having relatively loosely bound electrons or hetero atoms with lone pair of electrons. The pyrazolidine diones can be protonated in acid medium. According to Fouda *et al* (1986) mild steel surface bears a positive charge in sulphuric acid medium and it is very difficult for the protonated inhibitor molecules to approach positively charged mild steel surface due to electrostatic repulsion. However the protonated inhibitor molecule gets attached to the positively charged metal surface by means of electrostatic interaction between SO_4^{2-} of the medium and protonated pyrazolidine diones.

Analysis of the results obtained by all the three methods shows that the order of IE is BPP > PPD. This is due to the presence of phenyl ring attached with conjugated C=C which offers additional anchoring site for adsorption. This is also explained with HOMO-LUMO orbital pictures of the compounds. Analysis of Fig-12a shows that in PPD, the HOMO and LUMO densities were distributed over the entire molecule. Whereas in BPP, (Fig-12b) the HOMO densities were mainly located on phenylpyrazolidine moiety, i.e there is a high electron density around the phenyl group and the attached heterocyclic ring due to p- π conjugation. so this part would be preferentially adsorbed on the metal surface. The LUMO densities were concentrated on the other part i.e C₆H₅-C=C- and the LUMO orbitals also interact with metal by adsorbed on the metal surface forming a more protective film than PPD where the HOMO-LUMO are separated over the entire molecule. Similar results were reported by (Oguike *et al*, 2013).

Conclusion

The main conclusions drawn from this study are, the synthesized pyrazolidine diones inhibit the corrosion of mild steel in 1M H₂SO₄ medium and behaves as mixed type. Adsorption of inhibitors on the surface of mild steel in 1M H₂SO₄ obeys Langmuir's adsorption isotherm. Electrochemical studies show the formation of a barrier film. The inhibition efficiency of the inhibitors increases with increasing the inhibitor concentration and decreases with temperature.

References

- Granese S L, Rosales B M, Oviedo C & Zerbino J O, (1992), The inhibition action of heterocyclic nitrogen organic compounds on Fe and steel in HCl media, *Corros Sci*, 33, pp 1493.

- Subramaniam G, Balasubramaniam K & Shridhar P, (1990), 1,1'-Alkylene bis-pyridinium compounds as pickling inhibitors, *Corros Sci*, 30, pp 1019.
- Hettiarachchi S, Chain Y W, Wilson R B & Agarwala V S Jr, (1989), Macrocyclic corrosion-inhibitors for steel in acid chloride environments, *Corrosion*, 45, pp 30-34
- Stupnisek- Lisac E, Metikos-Hukovic M, Lencic D, Vorkapic-Furac J & Berkovic K, (1992), Structural investigation of N-arylpyrroles as iron corrosion inhibitors in hydrochloric acid, *Corrosion*, 48, pp 924-930
- Raicheva S N, Aleksiev B V & Sokolov E J, (1993), The effect of the chemical structure of some nitrogen- and sulphur-containing organic compounds on their corrosion inhibiting action, *Corros Sci*, 34, pp 343
- Harish Kumar and Sandeep Jain, (2013), Synthesis and antimicrobial evaluation of 4-benzylidene-pyrazolidine-3, 5-dione derivatives, *Int.J.Pharm.Sci* 4(1), pp 453-4
- HuiCang, Wenyan Shi, Jinling Shao, Qi Xu, (2012), Study on the Pyrazole Corrosion Inhibition and Synergistic Effect for Copper in Alkaline Solution, *Int. J. Electrochem. Sci.*, 7, pp 5626 – 5632.
- Mehdi Ebadi, Wan Jeffrey Basirun, Hamid Khaledi and HapipahMohd Ali, (2012), Corrosion inhibition properties of pyrazolylindolenine compounds on copper surface in acidic media, *Ebadi et al. Chemistry Central Journal*, 6, pp 163.
- L. Herrag, A. Chetouani, S. Elkadiri, B. Hammouti, A. Aouniti, (2008), Pyrazole Derivatives as Corrosion Inhibitors for Steel in Hydrochloric Acid, *PortugaliaeElectrochimicaActa*, 26, pp 211-220
- Ali S A, Saeed M T, and Rahman S U, (2003), The isoxazolidines: a new class of corrosion inhibitors of mild steel in acidic medium, *Corros Sci*, 45, pp 253-266
- Prabhu R A, Venkatesa T V, Shanbhag A V, Kulkarni G M, Kalkhambkar R G, (2008), Inhibition effects of some Schiff's bases on the corrosion of mild steel in hydrochloric acid solution, *Corros.Sci*, 50, pp 3356-3362
- Umoren S A, Ebenso E E, (2007), The synergistic effect of polyacrylamide and iodide ions on the corrosion inhibition of mild steel in H₂SO₄, *Mater. Chem. Phys.*, 106, pp 387-39
- H.E. El Ashry, A.ElNemr, S.A.Esawy, S.Ragab, (2006), Corrosion Inhibitors: Part II: Quantum Chemical Studies on the Corrosion Inhibitions of Steel in Acidic Medium by Some Triazole, Oxadiazole and Thiadiazole Derivatives, *ElectrochimicaActa* 51, pp 3957-396
- Obi-Egbedi NO, Obot IB, El-Khaiary MI, Umoren SA and Ebenso EE, (2011), Computational Simulation and Statistical Analysis on the Relationship Between Corrosion Inhibition Efficiency and Molecular Structure of Some Phenanthroline Derivatives on Mild Steel Surface, *Int.J.Electrochem.Sci.*, 6, pp 5649-567
- Ebenso EE, isabirye DA and Eddy NO, (2010), Adsorption and Quantum Chemical Studies on the Inhibition Potentials of Some Thiosemicarbazides for the Corrosion of Mild Steel in Acidic Medium, *Int.J.Mol.Sci.*, 11, pp 2473-249
- Hasanon R, Sadikglu M and Bilgic S, (2007), Electrochemical and quantum chemical studies of some Schiff bases on the corrosion of steel in H₂SO₄ solution, *Appl.Surf.Sci.*, 253, pp 3913-392
- H.M.Bhajiwala, R.T.vashi, I Bull. (2001), Ethanolamine, diethanolamine and triethanolamine as corrosion inhibitors for zinc in binary acid mixture [HNO₃+H₃PO₄], *Electrochem*, 17, pp 441-44
- A.Fouda, M.Moussa, F.I.Taha, A.I. ElNeanaa, (1986), The role of some thio semicarbazide derivatives in the corrosion inhibition of aluminium in hydrochloric acid, *Corros.Sci*, 26, pp 719-7
- R.S.Oguike, A.M.Kolo, A.M.Shibdawa, H.Y.Gyenna, (2013), Density Functional Theory of Mild Steel Corrosion in Acidic Media Using Dyes as Inhibitor: Adsorption onto Fe(110) from Gas Phase, *ISRN Physical chem*, Article ID 175910.